AD-A105 598 MARYLAND UNIV COLLEGE PARK SCHOOL OF ENGINEERING F/G 20/11
STRESS DISTRIBUTION AROUND A CIRCULAR HOLE IN SQUARE PLATES, LO--ETC(U)
SEP 81 M ERICKSON, A J DURELLI, K RAJAIAH N00014-81-K-0186
UNCLASSIFIED 55 NL

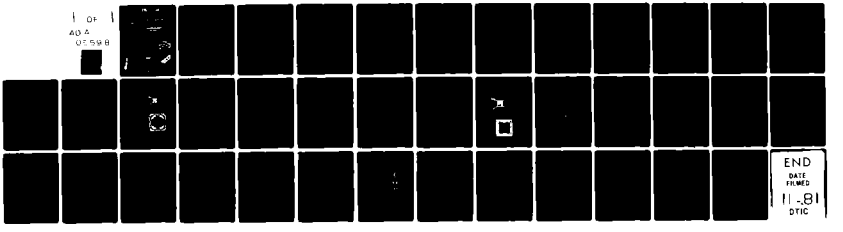

REPORT No. 55

STRESS DISTRIBUTION AROUND A CIRCULAR HOLE IN SQUARE PLATES, LOADED UNIFORMLY IN THE PLANE, ON TWO OPPOSITE SIDES OF THE SQUARE.

[redacted]

[redacted]

OPTIMUM SHAPES OF CENTRAL HOLES IN SQUARE PLATES SUBJECTED TO UNIAXIAL UNIFORM LOAD.

[redacted]

[redacted]

OPTIMIZATION OF HOLE SHAPES IN CIRCULAR CYLINDRICAL SHELLS UNDER AXIAL TENSION

BY K. RAJAIAH AND A. J. DURELLI

55
56

SPONSORED BY

OFFICE OF NAVAL RESEARCH
DEPARTMENT OF THE NAVY
WASHINGTON, D.C. 20025

M. /Erickson A. J. /Durelli
K./Rajaiah

ON
CONTRACT No. N00014-81-K-0186
U.M. PROJECT No. SF-CARS

SEP [redacted] 81

39

SCHOOL OF ENGINEERING
UNIVERSITY OF MARYLAND
COLLEGE PARK, MD. 20742

OPTIMIZATION OF THE SHAPE OF A HOLE IN A SQUARE PLATE AND IN A CIRCULAR SHELL

REPORTS 55, 56 AND 57

The following three reports are being distributed together and reprints of the papers previously published with their texts, in scientific journals, are used for the purpose. Circumstantial reasons, primarly cost, made this procedure advisable. One of the reports (56) deals with the optimization of the shape of an origionally circular hole present in a square plate, loaded uniformly and uniaxially in its plane. A second report (57) deals with the optimization of the shape of the hole, when the hole is present in a cylindrical shell subjected to axial tension. The third report (55) deals with the necessary background for the optimization of the hole in the square plate.

The abstracts of the previously published reports, prepared with O.N.R. support, are presented only once, before the text of the three present reports. The O.N.R. reports distribution list is also presented only once, at the end. A Report Documentation Page follows each individual report.

Previous Technical Reports to the Office of Naval Research

1. A. J. Durelli, "Development of Experimental Stress Analysis Methods to Determine Stresses and Strains in Solid Propellant Grains"--June 1962.
Developments in the manufacturing of grain-propellant models are reported. Two methods are given: a) cementing routed layers and b) casting.

2. A. J. Durelli and V. J. Parks, "New Method to Determine Restrained Shrinkage Stresses in Propellant Grain Models"--October 1962.
The birefringence exhibited in the curing process of a partially restrained polyurethane rubber is used to determine the stress associated with restrained shrinkage in models of solid propellant grains partially bonded to the case.

3. A. J. Durelli, "Recent Advances in the Application of Photoelasticity in the Missile Industry"--October 1962.
Two- and three-dimensional photoelastic analysis of grains loaded by pressure and by temperature are presented. Some applications to the optimization of fillet contours and to the redesign of case joints are also included.

4. A. J. Durelli and V. J. Parks, "Experimental Solution of Some Mixed Boundary Value Problems"--April 1964.
Means of applying known displacements and known stresses to the boundaries of models used in experimental stress analysis are given. The application of some of these methods to the analysis of stresses in the field of solid propellant grains is illustrated. The presence of the "pinching effect" is discussed.

5. A. J. Durelli, "Brief Review of the State of the Art and Expected Advance in Experimental Stress and Strain Analysis of Solid Propellant Grains"--April 1964.
A brief review is made of the state of the experimental stress and strain analysis of solid propellant grains. A discussion of the prospects for the next fifteen years is added.

6. A. J. Durelli, "Experimental Strain and Stress Analysis of Solid Propellant Rocket Motors"--March 1965.
A review is made of the experimental methods used to strain-analyze solid propellant rocket motor shells and grains when subjected to different loading conditions. Methods directed at the determination of strains in actual rockets are included.

7. L. Ferrer, V. J. Parks and A. J. Durelli, "An Experimental Method to Analyze Gravitational Stresses in Two-Dimensional Problems"--October 1965.
Photoelasticity and moiré methods are used to solve two-dimensional problems in which gravity-stresses are present.

8. A. J. Durelli, V. J. Parks and C. J. del Rio, "Stresses in a Square Slab Bonded on One Face to a Rigid Plate and Shrunk"--November 1965.
A square epoxy slab was bonded to a rigid plate on one of its faces in the process of curing. In the same process the photoelastic effects associated with a state of restrained shrinkage were "frozen-in." Three-dimensional photoelasticity was used in the analysis.

9. A. J. Durelli, V. J. Parks and C. J. del Rio, "Experimental Determination of Stresses and Displacements in Thick-Wall Cylinders of Complicated Shape"--April 1966.
Photoelasticity and moiré are used to analyze a three-dimensional rocket shape with a star shaped core subjected to internal pressure.

10. V. J. Parks, A. J. Durelli and L. Ferrer, "Gravitational Stresses Determined Using Immersion Techniques"--July 1966.
The methods presented in Technical Report No. 7 above are extended to three-dimensions. Immersion is used to increase response.

11. A. J. Durelli and V. J. Parks. "Experimental Stress Analysis of Loaded Boundaries in Two-Dimensional Second Boundary Value Problems"--February 1967.
The pinching effect that occurs in two-dimensional bonding problems, noted in Reports 2 and 4 above, is analyzed in some detail.

12. A. J. Durelli, V. J. Parks, H. C. Feng and F. Chiang, "Strains and Stresses in Matrices with Inserts,"-- May 1967.
Stresses and strains along the interfaces, and near the fiber ends, for different fiber end configurations, are studied in detail.

13. A. J. Durelli, V. J. Parks and S. Uribe, "Optimization of a Slot End Configuration in a Finite Plate Subjected to Uniformly Distributed Load,"--June 1967.
Two-dimensional photoelasticity was used to study various elliptical ends to a slot, and determine which would give the lowest stress concentration for a load normal to the slot length.

14. A. J. Durelli, V. J. Parks and Han-Chow Lee, "Stresses in a Split Cylinder Bonded to a Case and Subjected to Restrained Shrinkage,"--January 1968.
A three-dimensional photoelastic study that describes a method and shows results for the stresses on the free boundaries and at the bonded interface of a solid propellant rocket.

15. A. J. Durelli, "Experimental Stress Analysis Activities in Selected European Laboratories"--August 1968.
This report has been written following a trip conducted by the author through several European countries. A list is given of many of the laboratories doing important experimental stress analysis work and of the people interested in this kind of work. An attempt has been made to abstract the main characteristics of the methods used in some of the countries visited.

16. V. J. Parks, A. J. Durelli and L. Ferrer, "Constant Acceleration Stresses in a Composite Body"--October 1968.
Use of the immersion analogy to determine gravitational stresses in two-dimensional bodies made of materials with different properties.

17. A. J. Durelli, J. A. Clark and A. Kochev, "Experimental Analysis of High Frequency Stress Waves in a Ring"--October 1968.
A method for the complete experimental determination of dynamic stress distributions in a ring is demonstrated. Photoelastic data is supplemented by measurements with a capacitance gage used as a dynamic lateral extensometer.

18. J. A. Clark and A. J. Durelli, "A Modified Method of Holographic Interferometry for Static and Dynamic Photoelasticity"--April 1968.
A simplified absolute retardation approach to photoelastic analysis is described. Dynamic isopachics are presented.

19. J. A. Clark and A. J. Durelli, "Photoelastic Analysis of Flexural Waves in a Bar"--May 1969.
A complete direct, full-field optical determination of dynamic stress distribution is illustrated. The method is applied to the study of flexural waves propagating in a urethane rubber bar. Results are compared with approximate theories of flexural waves.

20. J. A. Clark and A. J. Durelli, "Optical Analysis of Vibrations in Continuous Media"--June 1969.
Optical methods of vibration analysis are described which are independent of assumptions associated with theories of wave propagation. Methods are illustrated with studies of transverse waves in prestressed bars, snap loading of bars and motion of a fluid surrounding a vibrating bar.

21. V. J. Parks, A. J. Durelli, K. Chandrashekhara and T. L. Chen, "Stress Distribution Around a Circular Bar, with Flat and Spherical Ends, Embedded in a Matrix in a Triaxial Stress Field"--July 1969.
A Three-dimensional photoelastic method to determine stresses in composite materials is applied to this basic shape. The analyses of models with different loads are combined to obtain stresses for the triaxial cases.

22. A. J. Durelli, V. J. Parks and L. Ferrer, "Stresses in Solid and Hollow Spheres Subjected to Gravity or to Normal Surface Tractions"--October 1969.
The method described in Report No. 10 above is applied to two specific problems. An approach is suggested to extend the solutions to a class of surface traction problems.

23. J. A. Clark and A. J. Durelli, "Separation of Additive and Subtractive Moiré Patterns"--December 1969.
A spatial filtering technique for adding and subtracting images of several gratings is described and employed to determine the whole field of Cartesian shears and rigid rotations.

24. R. J. Sanford and A. J. Durelli, "Interpretation of Fringes in Stress-Holo-Interferometry"--July 1970.
Errors associated with interpreting stress-holo-interferometry patterns as the superposition of isopachics (with half order fringe shifts) and isochromatics are analyzed theoretically and illustrated with computer generated holographic interference patterns.

25. J. A. Clark, A. J. Durelli and P. A. Laura, "On the Effect of Initial Stress on the Propagation of Flexural Waves in Elastic Rectangular Bars"--December 1970.
Experimental analysis of the propagation of flexural waves in prismatic, elastic bars with and without prestressing. The effects of prestressing by axial tension, axial compression and pure bending are illustrated.

26. A. J. Durelli and J. A. Clark, "Experimental Analysis of Stresses in a Buoy-Cable System Using a Birefringent Fluid"--February 1971.
An extension of the method of photoviscous analysis is presented which permits quantitative studies of strains associated with steady state vibrations of immersed structures. The method is applied in an investigation of one form of behavior of buoy-cable systems loaded by the action of surface waves.

27. A. J. Durelli and T. L. Chen, "Displacements and Finite-Strain Fields in a Sphere Subjected to Large Deformations"--February 1972.
Displacements and strains (ranging from 0.001 to 0.50) are determined in a polyurethane sphere subjected to several levels of diametral compression. A 500 lines-per-inch grating was embedded in a meridian plane of the sphere and moiré effect produced with a non-deformed master. The maximum applied vertical displacement reduced the diameter of the sphere by 27 per cent.

28. A. J. Durelli and S. Machida, "Stresses and Strain in a Disk with Variable Modulus of Elasticity"--March 1972
A transparent material with variable modulus of elasticity has been manufactured that exhibits good photoelastic properties and can also be strain analyzed by moiré. The results obtained suggests that the stress distribution in the disk of variable E is practically the same as the stress distribution in the homogeneous disk. It also indicates that the strain fields in both cases are very different, but that it is possible, approximately, to obtain the stress field from the strain field using the value of E at every point, and Hooke's law.

29. A. J. Durelli and J. Buitrago, "State of Stress and Strain in a Rectangular Belt Pulled Over a Cylindrical Pulley"--June 1972.
Two- and three-dimensional photoelasticity as well as electrical strain gages, dial gages and micrometers are used to determine the stress distribution in a belt-pulley system. Contact and tangential stress for various contact angles and friction coefficients are given.

30. T. L. Chen and A. J. Durelli, "Stress Field in a Sphere Subjected to Large Deformations"--June 1972.
Strain fields obtained in a sphere subjected to large diametral compressions from a previous paper were converted into stress fields using two approaches. First, the concept of strain-energy function for an isotropic elastic body was used. Then the stress field was determined with the Hookean type natural stress-natural strain relation. The results so obtained were also compared.

31. A. J. Durelli, V. J. Parks and H. M. Hasseem, "Helices Under Load"--July 1973.
Previous solutions for the case of close coiled helical springs and for helices made of thin bars are extended. The complete solution is presented in graphs for the use of designers. The theoretical development is correlated with experiments.

32. T. L. Chen and A. J. Durelli, "Displacements and Finite Strain Fields in a Hollow Sphere Subjected to Large Elastic Deformations"--September 1973.
The same methods described in No. 27, were applied to a hollow sphere with an inner diameter one half the outer diameter. The hollow sphere was loaded up to a strain of 30 per cent on the meridian plane and a reduction of the diameter by 20 per cent.

33. A. J. Durelli, H. H. Hasseem and V. J. Parks, "New Experimental Method in Three-Dimensional Elastostatics"--December 1973.
A new material is reported which is unique among three-dimensional stress-freezing materials, in that, in its heated (or rubbery) state it has a Poisson's ratio which is appreciably lower than 0.5. For a loaded model, made of this material, the unique property allows the direct determination of stresses from strain measurements taken at interior points in the model.

34. J. Wolak and V. J. Parks, "Evaluation of Large Strains in Industrial Applications"--April 1974.
It was shown that Mohr's circle permits the transformation of strain from one axis of reference to another, irrespective of the magnitude of the strain, and leads to the evaluation of the principal strain components from the measurement of direct strain in three directions.

35. A. J. Durelli, "Experimental Stress Analysis Activities in Selected European Laboratories"--April 1975.
Continuation of Report No. 15 after a visit to Belgium, Holland, Germany, France, Turkey, England and Scotland.

36. A. J. Durelli, V. J. Parks and J. O. Bühler-Vidal, "Linear and Non-linear Elastic and Plastic Strains in a Plate with a Big Hole Loaded Axially in its Plane"--July 1975.
Strain analysis of the ligament of a plate with a big hole indicates that both geometric and material non-linearity may take place. The strain concentration factor was found to vary from 1 to 2 depending on the level of deformation.

37. A. J. Durelli, V. Pavlin, J. O. Bühler-Vidal and G. Ome, "Elastostatics of a Cubic Box Subjected to Concentrated Loads"--August 1975.
Analysis of experimental strain, stress and deflection of a cubic box subjected to concentrated loads applied at the center of two opposite faces. The ratio between the inside span and the wall thickness was varied between approximately 5 and 121.

38. A. J. Durelli, V. J. Parks and J. O. Bühler-Vidal, "Elastostatics of Cubic Boxes Subjected to Pressure"--March 1976.
Experimental analysis of strain, stress and deflections in a cubic box subjected to either internal or external pressure. Inside span-to-wall thickness ratio varied from 5 to 14.

39. Y. Y. Hung, J. D. Hovanesian and A. J. Durelli, "New Optical Method to Determine Vibration-Induced Strains with Variable Sensitivity After Recording"--November 1976.
A steady state vibrating object is illuminated with coherent light and its image slightly misfocused. The resulting specklegram is "time-integrated" as when Fourier filtered gives derivatives of the vibrational amplitude.

40. Y. Y. Hung, C. Y. Liang, J. D. Hovanesian and A. J. Durelli, "Cyclic Stress Studies by Time-Averaged Photoelasticity"--November 1976.
"Time-averaged isochromatics" are formed when the photographic film is exposed for more than one period. Fringes represent amplitudes of the oscillating stress according to the zeroth order Bessel function.

41. Y. Y. Hung, C. Y. Liang, J. D. Hovanesian and A. J. Durelli, "Time-Averaged Shadow Moiré Method for Studying Vibrations"--November 1976.
Time-averaged shadow moiré permits the determination of the amplitude distribution of the deflection of a steady vibrating plate.

42. J. Buitrago and A. J. Durelli, "On the Interpretation of Shadow-Moiré Fringes"--April 1977.
Possible rotations and translations of the grating are considered in a general expression to interpret shadow-moiré fringes and on the sensitivity of the method. Application to an inverted perforated tube.

43. J. der Hovanesian, "18th Polish Solid Mechanics Conference." Published in European Scientific Notes of the Office of Naval Research, in London, England, Dec. 31, 1976.
Comments on the planning and organization of, and scientific content of paper presented at the 18th Polish Solid Mechanics Conference held in Wisla-Jawornik from September 7-14, 1976.

44. A. J. Durelli, "The Difficult Choice,"--May 1977.
The advantages and limitations of methods available for the analyses of displacements, strain, and stresses are considered. Comments are made on several theoretical approaches, in particular approximate methods, and attention is concentrated on experimental methods: photo-elasticity, moiré, brittle and photoelastic coatings, gages, grids, holography and speckle to solve two- and three-dimensional problems in elasticity, plasticity, dynamics and anisotropy.

45. C. Y. Liang, Y. Y. Hung, A. J. Durelli and J. D. Hovanesian, "Direct Determination of Flexural Strains in Plates Using Projected Gratings,"--June 1977.
The method requires the rotation of one photograph of the deformed grating over a copy of itself. The moiré produced yields strains by optical double differentiation of deflections. Applied to projected gratings the idea permits the study of plates subjected to much larger deflections than the ones that can be studied with holograms.

46. A. J. Durelli, K. Brown and P. Yee, "Optimization of Geometric Discontinuities in Stress Fields"--March 1978.
The concept of "coefficient of efficiency" is introduced to evaluate the degree of optimization. An ideal design of the inside boundary of a tube subjected to diametral compression is developed which decreases its maximum stress by 25%, at the time it also decreases its weight by 10%. The efficiency coefficient is increased from 0.59 to 0.95. Tests with a brittle material show an increase in strength of 20%. An ideal design of the boundary of the hole in a plate subjected to axial load reduces the maximum stresses by 26% and increases the coefficient of efficiency from 0.54 to 0.90.

47. J. D. Hovanesian, Y. Y. Hung and A. J. Durelli, "New Optical Method to Determine Vibration-Induced Strains With Variable Sensitivity After Recording"--May 1978.
A steady-state vibrating object is illuminated with coherent light and its image is slightly misfocused in the film plane of a camera. The resulting processed film is called a "time-integrated specklegram." When the specklegram is Fourier filtered, it exhibits fringes depicting derivatives of the vibrational amplitude. The direction of the spatial derivative, as well as the fringe sensitivity may be easily and continuously varied during the Fourier filtering process. This new method is also much less demanding than holographic interferometry with respect to vibration isolation, optical set-up time, illuminating source coherence, required film resolution, etc.

48. Y. Y. Hung and A. J. Durelli, "Simultaneous Determination of Three Strain Components in Speckle Interferometry Using a Multiple Image Shearing Camera,"--September 1978
This paper describes a multiple image-shearing camera. Incorporating coherent light illumination, the camera serves as a multiple shearing speckle interferometer which measures the derivatives of surface displacements with respect to three directions simultaneously. The application of the camera to the study of flexural strains in bent plates is shown, and the determination of the complete state of two-dimensional strains is also considered. The multiple image-shearing camera uses an interference phenomena, but is less demanding than holographic interferometry with respect to vibration isolation and the coherence of the light source. It is superior to other speckle techniques in that the obtained fringes are of much better quality.

49. A. J. Durelli and K. Rajaiah, "Quasi-square Hole With Optimum Shape in an Infinite Plate Subjected to In-plane Loading"--January 1979. This paper deals with the optimization of the shape of the corners and sides of a square hole, located in a large plate and subjected to in-plane loads. Appreciable disagreement has been found between the results obtained previously by other investigators. Using an optimization technique, the authors have developed a quasi-square shape which introduces a stress concentration of only 2.54 in a uniaxial field, the comparable value for the circular hole being 3. The efficiency factor of the proposed optimum shape is 0.90. whereas the one of the best shape developed previously was 0.71. The shape also is developed that minimizes the stress concentration in the case of biaxial loading when the ratio of biaxiality is 1:-1.

50. A. J. Durelli and K. Rajaiah, "Optimum Hole Shapes in Finite Plates Under Uniaxial Load,"--February 1979.
This paper presents optimized hole shapes in plates of finite width subjected to uniaxial load for a large range of hole to plate widths (D/W) ratios. The stress concentration factor for the optimized holes decreased by as much as 44% when compared to circular holes. Simultaneously, the area covered by the optimized hole increased by as much as 26% compared to the circular hole. Coefficients of efficiency between 0.91 and 0.96 are achieved. The geometries of the optimized holes for the D/W ratios considered are presented in a form suitable for use by designers. It is also suggested that the developed geometries may be applicable to cases of rectangular holes and to the tip of a crack. This information may be of interest in fracture mechanics.

51. A. J. Durelli and K. Rajaiah, "Determination of Strains in Photoelastic Coatings,"--May 1979
Photoelastic coatings can be cemented directly to actual structural components and tested under field conditions. This important advantage has made them relatively popular in industry. The information obtained, however, may be misinterpreted and lead to serious errors. A correct interpretation requires the separation of the principal strains and so far, this operation has been found very difficult. Following a previous paper by one of the authors, it is proposed to drill small holes in the coating and record the birefringence at points removed from the edge of the holes. The theoretical background of the method is reviewed; the technique necessary to use it is explained and two applications are described. The precision of the method is evaluated and found satisfactory in contradiction to information previously published in the literature.

52. A. J. Durelli and K. Rajaiah, "Optimized Inner Boundary Shapes in Circular Rings Under Diametral Compression,"--June 1979.
Using a method developed by the authors, the configuration of the inside boundary of circular rings, subjected to diametral compression, has been optimized, keeping cleared the space enclosed by the original circular inside boundary. The range of diameters studied was $0.33 \leq ID/OD \leq 0.7$. In comparison with circular rings of the same ID/OD, the stress concentrations have been reduced by about 30%, the weight has been reduced by about 10% and coefficients of efficiency of about 0.96 have been attained. The maximum values of compressive and tensile stresses on the edge of the hole, are approximately equal, there are practically no gradients of stress along the edge of the hole, and sharp corners exhibit zero stress. The geometries for each ID/OD design are given in detail.

53. A. J. Durelli and K. Rajaiah, "Lighter and Stronger,"--February 1980.
A new method has been developed that permits the direction design of shapes of two-dimensional structures and structural components, loaded in their plane, within specified design constrains and exhibiting optimum distribution of stresses. The method uses photoelasticity and requires a large field diffused light polariscope. Several problems of optimization related to the presence of holes in finite and infinite plates, subjected to uniaxial and biaxial loadings, are solved parametrically.
Some unexpected results have been found: 1) the optimum shape of a large hole in a bar of finite width, subjected to uniaxial load, is "quasi" square, but the transverse boundary has the configuration of a "hat"; 2) for the small hole in the large plate, a "barrel" shape has a lower s.c.f. than the circular hole and appreciably higher coefficient of efficiency; 3) the optimum shape of a tube, subjected to diametral compression, has small "hinges" and is much lighter and stronger than the circular tube. Applications are also shown to the design of dove-tails and slots in turbine blades and rotors, and to the design of star-shaped solid propellant grains for rockets.

54. C. Brémond and A. J. Durelli, "Experimental Analysis of Displacements and Shears at the Surface of Contact Between two Loaded Bodies,"--July 1980.
The displacements which exist at the contact between two loaded bodies depend on the geometry of the surface of contact, the type of the loading and the property of the materials. A method has been developed to determine these displacements experimentally. A grid has been photographically printed on an interior plane of a transparent model of low modulus of elasticity. The displacements were recorded photographically and the analysis was conducted on the photographs of the deformed grids. Shears were determined from the change in angles. The precision of the measurements at the interface is estimated to be plus or minus 0.05mm. Examples of application are given for the cases of loads applied normally and tangentially to a rigid cylindrical punch resting on a semi-infinite solft plate. Important observations can be made on the zones of friction and of slip. The proposed method is three-dimensional and the distributions can be obtained at several interior planes by changing the position of the plane of the grid. The limitations of the method are pointed out. The possibility of using gratings (12 to 40 lpmm) is considered as well as the advantages of using moiré to analyze the displacements.

55. M. Erickson and A. J. Durelli, "Stress Distribution Around a Circular Hole in Square Plates, Loaded Uniformly in the Plane, on two Opposite Sides of the Square"--The complete stress distribution around a circular hole, located in the center of a square plate, has been determined photoelastically for the case of the plate loaded uniformly on two opposite sides. The study was conducted parametrically for a large range of the ratio of the side of the square to the diameter of the hole. The results obtained permit the determination of the stresses for any biaxial condition and verify a previous solution obtained for the case of the pressurized hole. The experimental procedure is briefly described.

56. A. J. Durelli, M. Erickson and K. Rajaiah, " "This paper presents the shapes that will optimize the stress distribution about central holes in square plates subjected to uniform load on two opposite sides of the plate. The study is conducted for a large range of hole to plate widths ratios (D/W). The stress concentration factor for the optimized holes decreased by as much as 21% when compared to the one associated with a circular hole. Simultaneously, the weight of the plate with optimized hole is reduced by as much as 36% as compared to the circular hole. Coefficient of efficiecy of around 0.92 is achieved for all D/W ratios. The geometry of the optimized holes are presented in a form suitable for use by designers.

STRESS DISTRIBUTION AROUND A CIRCULAR HOLE IN SQUARE PLATES, LOADED UNIFORMLY IN THE PLANE, ON TWO OPPOSITE SIDES OF THE SQUARE

by

M. Erickson and A. J. Durelli

Sponsored by

Office of Naval Research
Department of the Navy
Washington, D.C. 20025

on

Contract No. N00014-81-K-0186
U.M. Project No. SF-CARS

Report No. 55

School of Engineering
University of Maryland
College Park, Md. 20742

STRESS DISTRIBUTION AROUND A CIRCULAR HOLE IN SQUARE PLATES, LOADED UNIFORMLY IN THE PLANE, ON TWO OPPOSITE SIDES OF THE SQUARE

by M. Erickson and A. J. Durelli

TABLE OF CONTENTS

ABSTRACT . . . . . .

INTRODUCTION . . . . . .

TEST PROCEDURE . . . . . .

ACKNOWLEDGMENTS . . . . . .

REFERENCES . . . . . .

Stress Distribution Around a Circular Hole in Square Plates, Loaded Uniformly in the Plane, on Two Opposite Sides of the Square

M. Erickson[1] and A. J. Durelli[2]

The complete stress distribution around a circular hole, located in the center of a square plate, has been determined photoelastically for the case of the plate loaded uniformly on two opposite sides. The study was conducted parametrically for a range of the ratio D/W of the diameter of the hole to the side of the square from 0.20 to 0.83. The results obtained permit the determination of the stresses for any biaxial condition and verify a previous solution obtained for the case of the pressurized hole. The experimental procedure is briefly described.

Introduction

The classical problem of the stress distribution around a circular hole in an infinite plate subjected to a uniaxial uniform loading in the plane of the plate was solved by Kirsch [1] in closed form. The appreciably more complicated case of the finite plate with the circular hole was solved by Howland [2] using an infinite series solution, but results were evaluated only for $D/W < 0.5$, D being the diameter of the hole and W the width of the plate. The distribution of stress for the cases when $D/W > 0.5$ was obtained experimentally by Wahl and Beeuwkes [3]. The stress-concentration factors referred to both the gross area and the net area, for the total range of D/W values are given in [4]. The case of the very large hole in the plate, when D/W approaches one presented some problems of interpretation, which have been dealt with in [5].

The stress distribution for the case of a square plate with a circular hole was solved experimentally [6] when a uniform pressure is applied inside the hole, or what is equivalent [7], when the four sides of the square are subjected to uniform pressure. The problem of the square plate with a circular hole, subjected to in-plane uniform pressure applied to two opposite sides of the plate, has not been solved. The problem is important and if the solution were available, the solution of the previously mentioned problem for any ratio of biaxiality could be obtained as a special case by superposition. That is the problem dealt with in this Note. The solution is obtained photoelastically for a range of D/W values from 0.20 to 0.83.

Test Procedure

The analysis was conducted in a 3-in-sq, $\frac{1}{4}$-in-thick (Homalite 100)

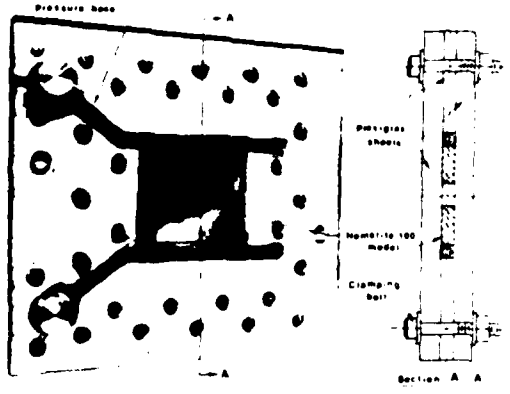

Fig. 1 Loading device used to apply uniform pressure to two opposite sides of a square plate

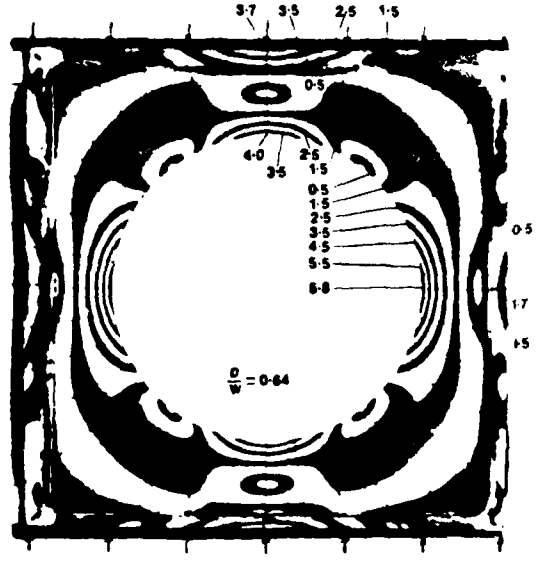

Fig. 2 Typical isochromatic pattern around a circular hole in a square plate subjected to uniform pressure on two opposite sides

[1] Adjunct Professor, School of Engineering, Oakland University, Rochester, Mich. 48063.

[2] Professor, Department of Mechanical Engineering, University of Maryland, College Park, Md 20742. Fellow ASME.

Manuscript received by ASME Applied Mechanics Division, April, 1980, final revision, October, 1980.

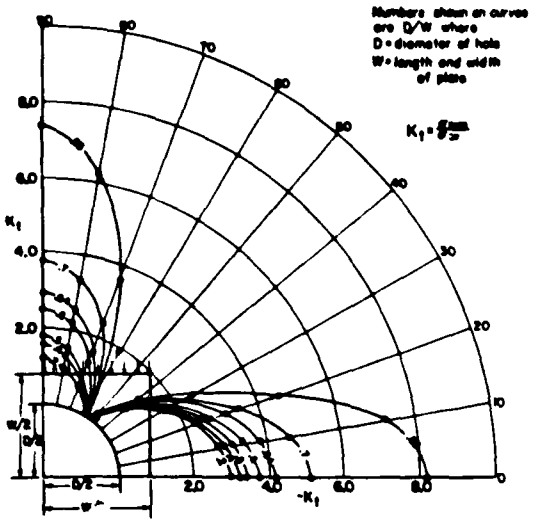

Fig. 3 K_t as distributions on inner boundary of a round hole in a square plate subjected to uniform pressure on two opposite sides (average stress on the net section used for comparison)

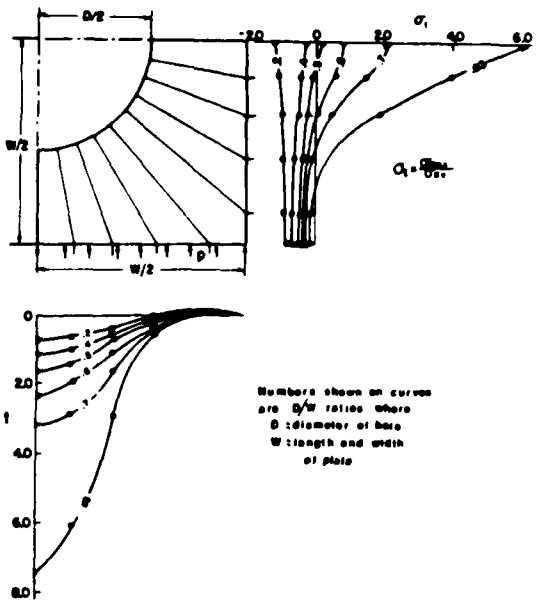

Fig. 4 Stress distributions on outer boundary of a square plate with a round hole subjected to uniform pressure applied to two opposite sides of the plate (average stress on the net section used for comparison)

specimen (Fig. 1). The uniform pressure is applied by means of a specially built device as described in [8]. Two rubber hoses, one placed on each of the opposite sides of the plate are used. The deformation of the pressurized hose is restrained by Plexiglass sheets. The loading frame had to be calibrated to determine the amount of pressure actually applied to the specimen. For this purpose, a strain gaged load cell was specially designed. The average fringe order was computed using the applied pressure and the fringe value of the material and a check obtained by algebraically averaging the areas above and below the zero axis for those specimens with high D/W.

Seven specimens were used with the inner hole diameter varying from 0.6 in. to 2.5 in. giving D/W values from 0.2 to 0.83, where D is the hole diameter and W the width of the specimen. Dark field and light field photographs were taken in a diffused light polariscope of the seven specimens, subjected to pressure sufficient to produce a maximum of about 5 fringes (Fig. 2). Fractional fringe orders were recorded using Tardy's method of compensation at every 10° at the edge of the hole from 0° (horizontal) to 90° (vertical). Readings were also taken on the outer edge of the plate at the 0° and 90° points. A calibration test on a 2.5-in-dia round disk of the material gave a material constant of 156 lb/in./fringe.

The results obtained are given as stress distributions along the inside and the outside boundaries (Figs. 3 and 4), and as stress concentrations at the intersection of the longitudinal and transverse axes with the boundary of the hole. All values are given parametrically as functions of D/W. These results permit, by superposition, the determination of stresses for any ratio of biaxial loading of the plate. The case of equal biaxiality was computed and is shown in Fig. 5. The values obtained verify those previously published for the case of the hydrostatically loaded hole [6], using the transformation explained in [7].

It may be noted that, in the present problem, K_t increases as D/W increases while for the case of circular holes in long rectangular plates, K_t decreases as D/W increases.

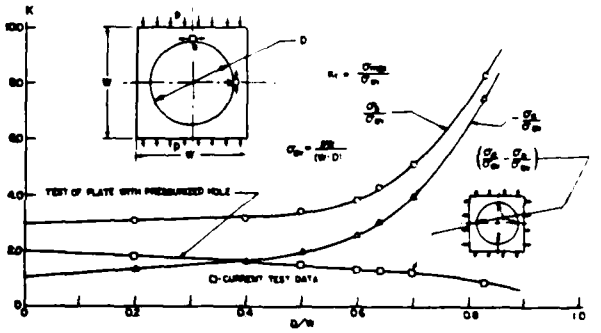

Fig. 5 Stress-concentration factors for a round hole in a square plate subjected to a uniaxial uniform pressure and computations for the biaxial case

Acknowledgments

The research program from which this Note was developed was supported, in part, by the Office of Naval Research (Contract No. N00014-76-C-0487). The authors are grateful to N. Perrone and N. Basdekas of ONR for their support. The photoelastic specimens have been prepared by S. Nygren and the manuscript reproduction by P. Baxter.

References

1 Kirsch G., "Die Theorie der Elastizitaet and die Bedueerfnisse der Festigkeitlehre," *Z. Ver. deut. Ing. W.*, Vol. 32, 1898, pp. 797–807.

2 Howland C. J., "On the Stresses in the Neighborhood of a Circular Hole in a Strip Under Tension," *Transactions of the Royal Society*, London, Series A, Vol. 229, 1929–1930, pp. 49–86.

3 Wahl, M., and Beeuwkes, R., "Stress Concentration Produced by Holes and Notches," ASME TRANS., Vol. 56, Aug. 1934, pp. 617–623.

4 Durelli A. J., Phillips, E. A., and Tsao, C. J., *Introduction to the Theoretical and Experimental Analysis of Stress and Strain*, McGraw-Hill, New York, 1958.

5 Durelli A. J., Parks, V. J., and Buhler-Vidal, J. O., "Linear and Nonlinear Elastic and Plastic Strains in a Plate With a Large Hole Loaded Axially in Its Plane," *International Journal of Nonlinear Mechanics*, Vol. 11, pp. 207–211.

6 Riley, W. F., Durelli, A. J., and Theocaris, P. S., "Further Stress Studies on a Square Plate With a Pressurized Central Circular Hole," *Proceedings of the 4th Midwestern Conference on Solid Mechanics*, Austin, Texas, Sept. 1959.

7 Parks, V. J., and Durelli, A. J., "Transfer of Hydrostatic Loading From One Boundary to Another," *Experimental Mechanics*, Vol. 15, No. 4, pp. 148–149, Apr. 1975.

8 Durelli A. J., *Applied Stress Analysis*, Prentice-Hall, Englewood Cliffs, N.J., 1967, pp. 78–79.

SECURITY CLASSIFICATION OF THIS PAGE (When Data Entered)

REPORT DOCUMENTATION PAGE		READ INSTRUCTIONS BEFORE COMPLETING FORM
1. REPORT NUMBER 55	2. GOVT ACCESSION NO. AD-A105598	3. RECIPIENT'S CATALOG NUMBER
4. TITLE (and Subtitle) STRESS DISTRIBUTION AROUND A CIRCULAR HOLE IN SQUARE PLATES, LOADED UNIFORMLY IN THE PLANE, ON TWO OPPOSITE SIDES OF THE SQUARE		5. TYPE OF REPORT & PERIOD COVERED 6. PERFORMING ORG. REPORT NUMBER
7. AUTHOR(s) M. Erickson and A. J. Durelli		8. CONTRACT OR GRANT NUMBER(s) N00014-81-K-0186
9. PERFORMING ORGANIZATION NAME AND ADDRESS University of Maryland College Park, Md.		10. PROGRAM ELEMENT, PROJECT, TASK AREA & WORK UNIT NUMBERS
11. CONTROLLING OFFICE NAME AND ADDRESS Office of Naval Research Dept. of the Navy Washington, D.C. 20025		12. REPORT DATE September 1981 13. NUMBER OF PAGES 9
14. MONITORING AGENCY NAME & ADDRESS(if different from Controlling Office)		15. SECURITY CLASS. (of this report) Unclassified 15a. DECLASSIFICATION/DOWNGRADING SCHEDULE

16. DISTRIBUTION STATEMENT (of this Report)

Distribution of this report is unlimited

17. DISTRIBUTION STATEMENT (of the abstract entered in Block 20, if different from Report)

18. SUPPLEMENTARY NOTES

19. KEY WORDS (Continue on reverse side if necessary and identify by block number)

Holes
Plates, square
Stress Concentrations
Photoelasticity

20. ABSTRACT (Continue on reverse side if necessary and identify by block number)

The complete stress distribution around a circular hole, located in the center of a square plate, has been determined photoelastically for the case of the plate loaded uniformly on two opposite sides. The study was conducted parametrically for a large range of the ratio of the side of the square to the diameter of the hole. The results obtained permit the determination of the stresses for any biaxial condition and verify a previous solution obtained for the case of the pressurized hole. The experimental procedure is briefly described.

DD FORM 1 JAN 73 1473 EDITION OF 1 NOV 65 IS OBSOLETE
S/N 0102-014-6601 |

SECURITY CLASSIFICATION OF THIS PAGE (When Data Entered)

OPTIMUM SHAPES OF CENTRAL HOLES IN SQUARE PLATES SUBJECTED TO UNIAXIAL UNIFORM LOAD

by

A. J. Durelli, M. Erickson and K. Rajaiah

Sponsored by

Office of Naval Research
Department of the Navy
Washington, D.C. 20025

on

Contract No. N00014-81-K-0186
U.M. Project No. SF-CARS

Report No. 56

School of Engineering
University of Maryland
College Park, Md. 20742

OPTIMUM SHAPES OF CENTRAL HOLES IN SQUARE PLATES SUBJECTED TO UNIAXIAL UNIFORM LOAD

by

A. . J. Durelli, M. Erickson and K. Rajaiah

TABLE OF CONTENTS

ABSTRACT . . . . . .

INTRODUCTION . . . . . .

OPTIMIZATION PROCEDURE . . . . . .

EXPERIMENTAL DETAILS . . . . . .

RESULTS . . . . . .

DISCUSSION . . . . . .

ACKNOWLEDGMENTS . . . . . .

REFERENCES . . . . . .

Int. J. Solids Structures Vol. 17, pp. 787–793, 1981
Printed in Great Britain

0020-7683/81/080787-07$02.00/0
Pergamon Press Ltd

OPTIMUM SHAPES OF CENTRAL HOLES IN SQUARE PLATES SUBJECTED TO UNIAXIAL UNIFORM LOAD

A. J. DURELLI, M. ERICKSON and K. RAJAIAH
Department of Mechanical Engineering, University of Maryland, College Park, MD 20742, U.S.A.

(*Received* 30 *June* 1980)

Abstract—This paper presents the shapes that will optimize the stress distribution about central holes in square plates subjected to uniform load on two opposite sides of the plate. The study is conducted for a large range of hole to plate widths ratios (D/W). The stress concentration factor for the optimized holes decreased by as much as 21% when compared to the one associated with a circular hole. Simultaneously, the weight of the plate with optimized hole is reduced by as much as 36% as compared to the circular hole. Coefficient of efficiency of around 0.92 is achieved for all D/W ratios. The geometry of the optimized holes are presented in a form suitable for use by designers.

INTRODUCTION

This paper is one in a series of papers dealing with the optimization of discontinuities in two dimensional stress fields. The optimum shape of a hole in an infinite plate subjected to uniaxial uniformly distributed load was presented in[1]. The shapes to be given to an optimized central hole in finite plates subjected to uniaxial uniform loading have been given in[2] for different ratios of the diameter of the hole to the width of the plate. The optimized inner boundary shapes of rings with circular outer boundaries subjected to diametral compression have been given in [3] for different ratios of outer to inner diameters. The description of the basic features of the method have been presented in[4, 5]. References to other contributions in the literature can be found in [5] among which the most important one is due to Heywood[6].

OPTIMIZATION PROCEDURE

The method consists in using photoelasticity, in a systematic way, to idealize a configuration so that its boundaries do not have gradients of stress along the length of the boundaries. In other words, the structure will have stresses uniformly, or almost uniformly distributed along the boundary. The procedure permits the direct design of the geometry of the structure rather than the conventional step by step design and analysis, satisfying the requirement that the maximum stress should be lower than an allowable stress and at the same time, the distribution should be as efficient as possible. The geometric constrains for the problem are stripulated initially. A transparent model of the structure is placed in a diffused light circular polariscope. (The material of the model should exhibit birefringence when under load and should be sufficiently sensitive to produce several fringes of interference.) The operator should be able to work on the model with a hand file or portable router at the same time that he looks at the model through the analyzer. The method requires that the operator file away material from the boundaries starting at the points where the stress (and therefore the fringe order) is at a minimum. The filing operation redistributes the fringes. The operator continues filing away material from the low stressed zones of the boundary until as much as possible of the length of the boundary shows the same order of birefringence. This is easy to detect because at that moment, the same fringe falls all along the length of the boundary. If the body has more than one boundary, it may be necessary to operate by steps back and forth from one boundary to the other. In some cases, white light may be more practical than monochromatic light, the objective being then to have the same color along the boundary.

The degree of optimization can be evaluated quantitatively by a coefficient of efficiency:

$$k_{eff} = \frac{1}{S_2 - S_0}\left(\frac{\int_{S_0}^{S_1} \sigma_t^{+}\,ds}{\sigma_{all}^{+}} + \frac{\int_{S_1}^{S_2} \sigma_t^{-}\,ds}{\sigma_{all}^{-}}\right)$$

where σ_t is the tangential stress, σ_{all} represents the maximum allowable stress (the positive and negative superscripts referring to tensile and compressive stresses, respectively), S_0 and S_1 are the limiting points of the segment of boundary subjected to tensile stresses and S_1 and S_2 are the limiting points of the segment of boundary with compressive stresses. The significance of the coefficient of efficiency was discussed in Refs. [2, 5]. The above criterion will be used in the present work to evaluate the optimized hole shapes. The design procedure will be particularly useful for components made with brittle materials, or components made with ductile materials subjected to fatigue.

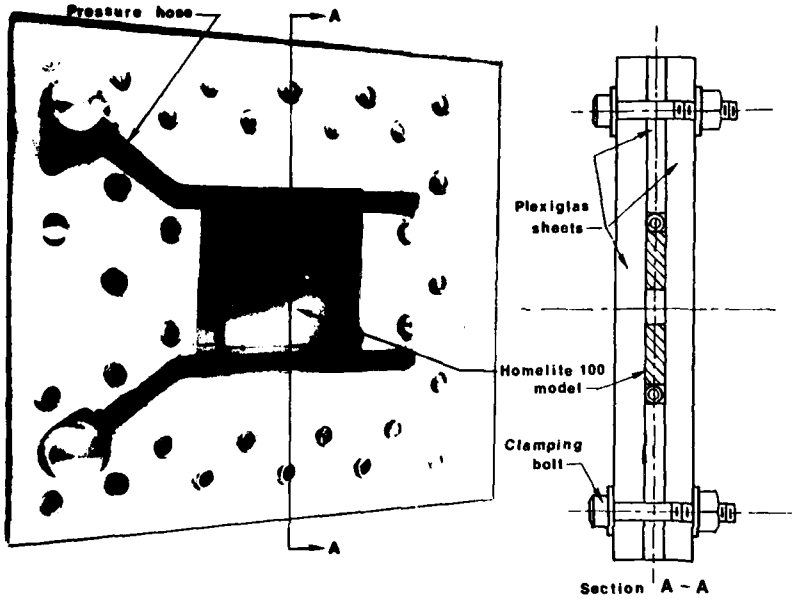

Fig. 1. Loading device used to apply uniform pressure to two opposite sides of a square plate.

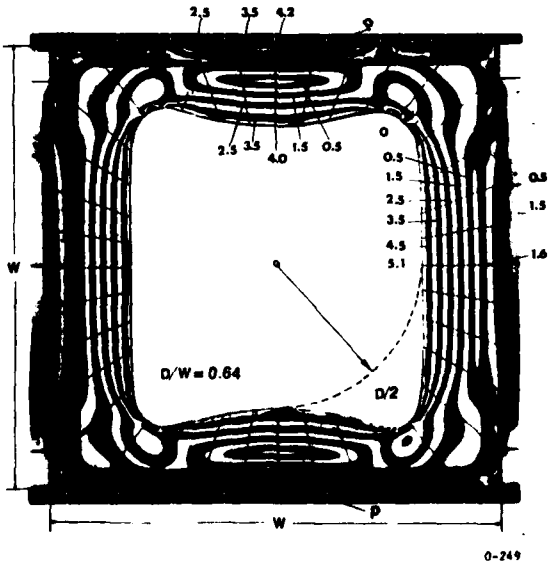

Fig. 2. Typical isochromatic pattern around an optimized hole in a square plate subjected to a uniaxial uniform pressure.

In this paper, using the technique described above, optimized hole shapes are presented in square plates subjected to uniaxial uniform compression.

EXPERIMENTAL DETAILS

Experiments were conducted with 0.23 in. (5.8 mm) thick Homalite-100 plates (fringe constant of 156 lb/in-fr (27.0 kN/m-fr)). The plate size was chosen as 3 × 3 in. (76.2 × 76.2 mm) for all D/W ratios. Optimization was carried out for $D/W = 0.20$; 0.41; 0.56; 0.65; 0.71; 0.79 and 0.89, with the models subjected to uniaxial uniformly distributed compression. Material was removed from the low stress regions by careful hand filing. To improve the precision, in particular at the corner zones, the operator used a binocular magnifier with a set of polarizer and quarter wave plates attached to each of its lenses, during the filing process. The uniform compression on the two parallel boundaries was applied following the methods developed previously[7, 8] and used recently in [9]. The position of a pressurized rubber tube located in the special device is shown in Fig. 1. This loading frame had to be calibrated to determine the

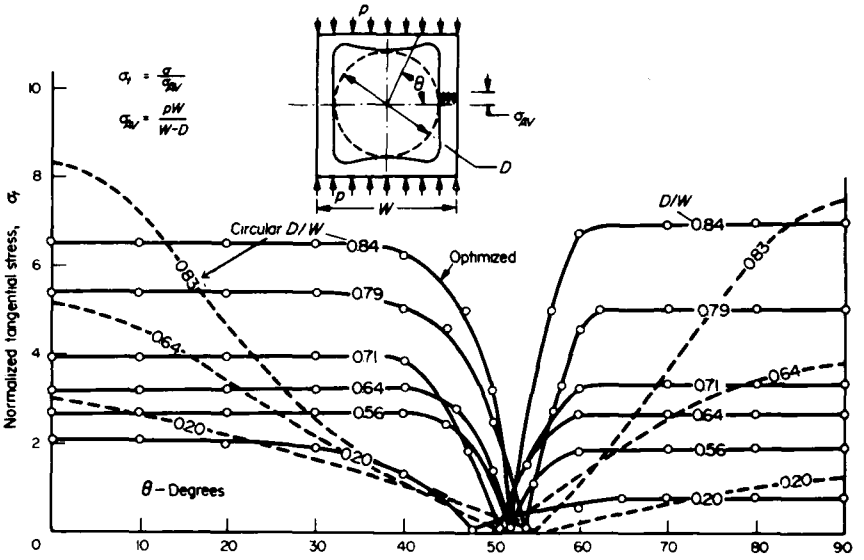

Fig. 3. Stress ratios for points on the boundary of optimized circular holes in a square plate subjected to uniaxial uniform pressure.

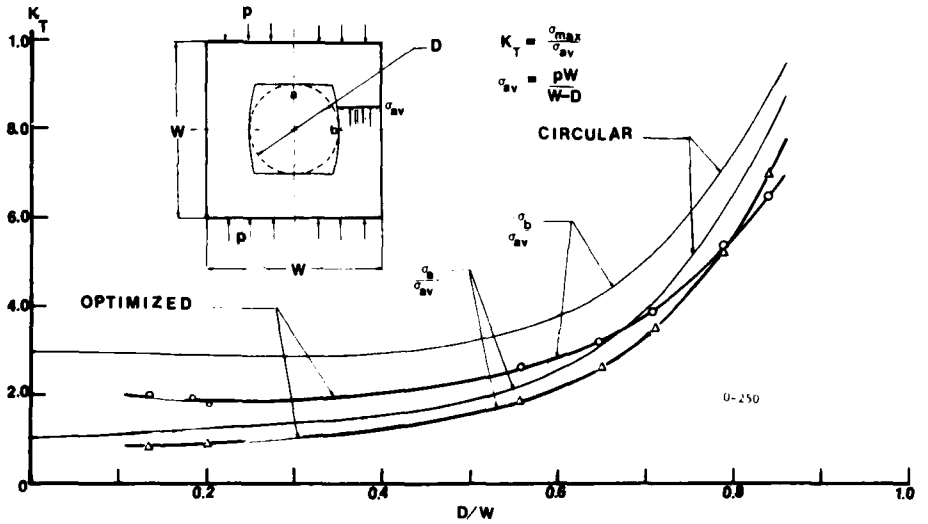

Fig. 4. Comparison of stress concentration factors for an optimized hole vs a circular hole in a square plate subjected to uniaxial uniform pressure.

amount of pressure actually applied to the specimen. For this purpose, a strain gaged load cell was specially designed.

RESULTS

The isochromatic pattern for a typical hole shape is shown in Fig. 2. The stress distributions around circular and optimized holes for the D/W ratios considered are presented in Fig. 3. The s.c.f. for the tensile and compressive regions of the circular and optimized holes for different D/W ratios are plotted in Fig. 4. The information on coefficient of efficiency and percentage weight reduction achieved are given in Fig. 5. The stress distributions on the outer edges are shown in Fig. 6.

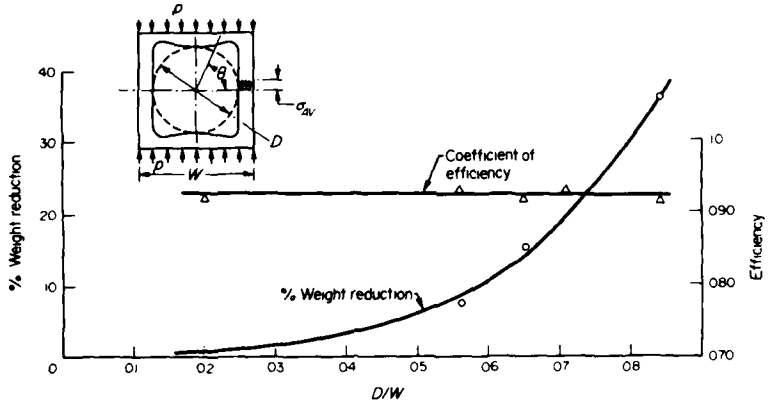

Fig. 5. Percentage weight reduction and coefficient of efficiency for an optimized hole in a square plate subjected to a uniaxial uniform pressure.

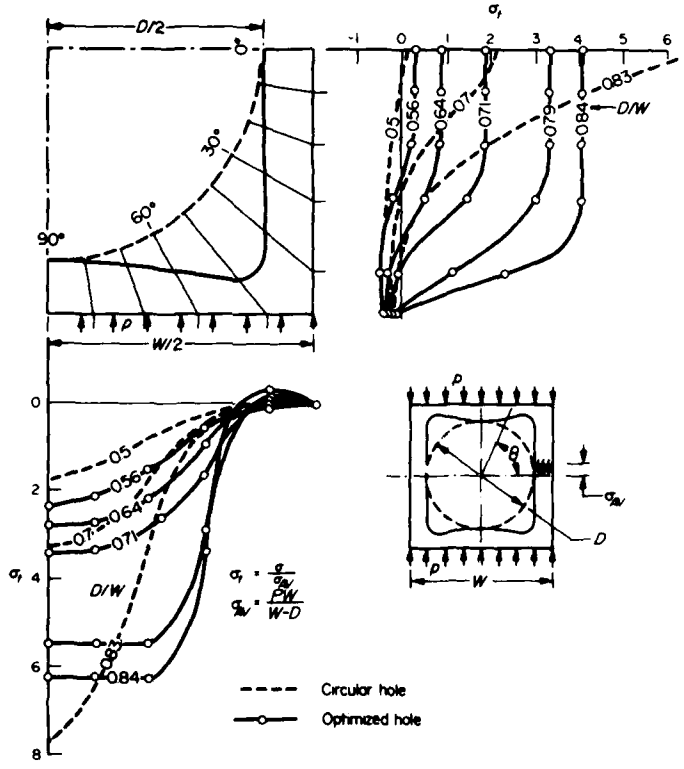

Fig. 6. Stress distribution along the outer boundaries of a square plate, with an optimized hole, subjected to uniform pressure on two opposite sides.

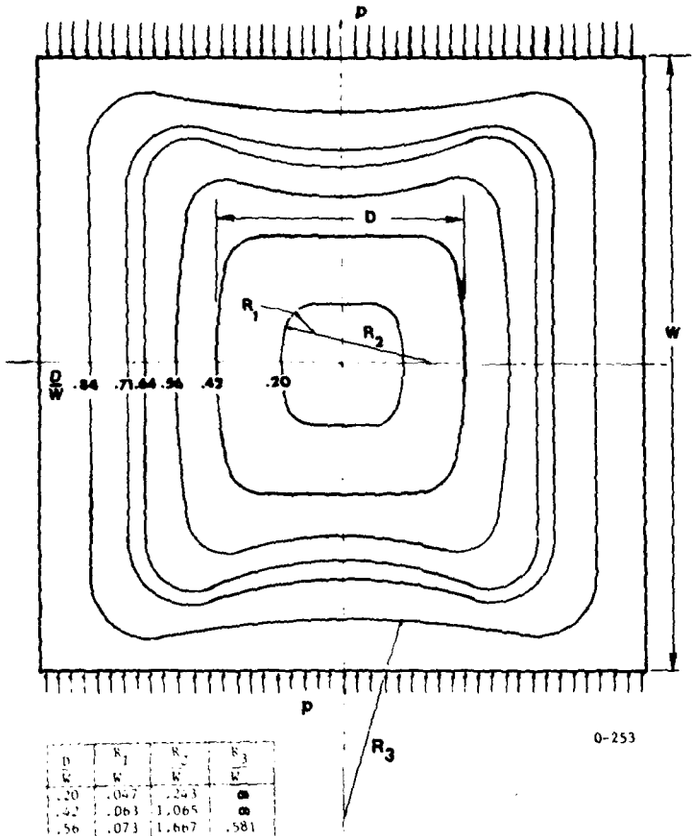

D/W	R1/W	R2/W	R3/W
.20	.047	.243	∞
.42	.063	1.065	∞
.56	.073	1.667	.581
.64	.080	∞	.557
.71	.084	∞	.710
.84	.093		1.580

Fig. 7. Optimum shape of a central hole in a square plate subjected to uniform pressure on two opposite sides (as function of D/W).

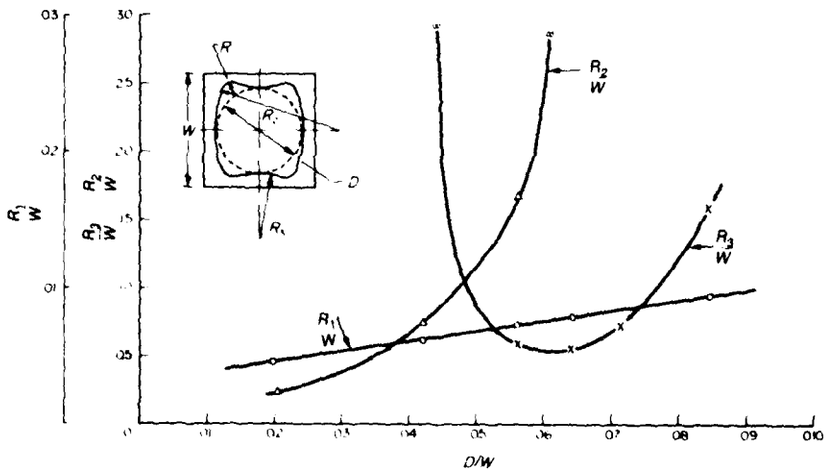

Fig. 8. Radii of the elements of holes producing optimum distribution of stress in square plates subjected to uniaxial uniform pressure.

The experimentally developed optimum hole geometries have been fitted with a combination of circles of different diameters and common tangents at the points of intersection. The hole geometries for the different D/W ratios are given in Fig. 7. The information given in Fig. 7 is consolidated in Fig. 8 in a graphical form to make easy its application.

DISCUSSION

The isochromatic pattern in Fig. 2 shows that the newly developed hole shape exhibits a high degree of optimization with the stresses remaining uniform along major portions of the tensile as well as compressive segments of the boundary. The information in Figs. 3 and 4 shows that, as compared to the circular holes, the optimum shapes have lead to significant reduction in s.c.f., the reduction ranging from 16% for $D/W = 0.14$ to about 21% for $D/W = 0.84$.

A coefficient of efficiency of about 0.92 has been achieved for all D/W ratios, as seen from Fig. 5. The optimum shapes have also lead to significant reduction in weight as compared to the circular holes, in the range of 1% for $D/W = 0.14$ to 36% for $D/W = 0.84$.

Comparison of the optimized shapes and the s.c.f. presented here for square plates with those given in Ref. [2] for long rectangular plates under identical loading conditions (except for the reversal of sign) brings out certain interesting features.

For $D/W < 0.3$, the optimized shapes are found to be identical, whereas for $D/W > 0.3$, the two shapes tend to become quite different especially on the hole edges perpendicular to the load axis. As D/W becomes larger, the hole shapes in square plates are predominantly influenced by the bending effect of the horizontal segments. No such bending effect can be observed in long rectangular plates.

For a very large value of D/W, the problem can be considered as that of a portal frame subjected to uniform load on top. The optimum shape presented can be taken as the shape to be given to a stress optimized portal frame.

While the s.c.f. for square plates decreases initially slightly and then increases monotonically with increase in D/W (Fig. 4), it was found to decrease monotically for long rectangular plates as D/W increases. For a given D/W ratio beyond $D/W = 0.5$, the s.c.f. for square plates is found to be very much higher than that for long rectangular plates. The reason for this increase can be traced to the behavior of the square plate as a portal frame, which increases appreciably the bending stresses in both the vertical and horizontal members.

For large D/W, the vertical elements of the plate become thinner and the fringes are not only parallel to the inner, but also to a large extent, to the outer boundaries indicating a linear variation of stress across the section. It also shows that, for large D/W, as the inner edge gets optimized, the outer edge also tends to become optimum. The distribution of stresses on the outer edges shown in Fig. 6 confirms this. It is also seen from Fig. 6 that the stress distribution becomes favorable also on the loaded edges with the tangential stresses remaining constant over a considerable length.

It is also seen from Fig. 4 that the location of maximum stress shifts from the vertical edge to the horizontal edge for $D/W > 0.81$.

Acknowledgements—The research program from which this paper was developed was supported, in part, by the Office of Naval Research (Contact No. N00014-76-C-0487). The authors are grateful to N. Perrone and N. Basdekas of ONR for this support. The photoelastic specimens have been prepared by S. Nygren and the manuscript reproduction by P. Baxter.

REFERENCES

1. A. J. Durelli and K. Rajaiah, Quasi-square hole with optimum shape in an infinite plate subjected to in-plane loading. *ONR Rep. No.* 49, Oakland University (Jan. 1979). To appear in the *J. Mech. Design* (A.S.M.E.).
2. A. J. Durelli and K. Rajaiah, Optimum hole shapes in finite plates under uniaxial load. *J. Appl. Mech.* **46**, 691–695 (Sept. 1979).
3. A. J. Durelli and K. Rajaiah, Optimized inner boundary shapes in circular rings under diametral compression. *Strain* 127–130 (Oct. 1979).
4. A. J. Durelli, K. Rajaiah, J. D. Hovanesian and Y. Y. Hung, General method of directly design stress-wise optimum two-dimensional structures. *Mech. Res. Comm.* **6**(3), 159–165 (1979).
5. A. J. Durelli, K. Brown and P. Yee, Optimization of geometric discontinuities in stress fields. *Exp. Mech.* **18**(8), 303–308 (Aug. 1978).

6. R. B. Heywood, *Designing by Photoelasticity*. Chapman & Hall, London (1958).
7. A. J. Durelli, Distribution of stresses in partial compression and a new method of determining the isostatics in photoelasticity. *Proc. 13th Semi-Annual Eastern Photoelasticity Conf.* pp. 25–50 (1941).
8. A. J. Durelli, Experimental means of analyzing stresses and strains in rocket propellant grains. *Exp. Mech.* 2(4), 102–110 (1962).
9. M. Erickson and A. J. Durelli, Stress distribution around a circular hole in square plates loaded uniformly in the plane on two opposite sides of the square. *ONR Rep. No.* 55, Oakland University (1980).

circular hole. Coefficient of efficiency of around 0.92 is achieved for all D/W ratios. The geometry of the optimized holes are presented in a form suitable for use by designers.

SECURITY CLASSIFICATION OF THIS PAGE (When Data Entered)

REPORT DOCUMENTATION PAGE		READ INSTRUCTIONS BEFORE COMPLETING FORM
1. REPORT NUMBER: 56	2. GOVT ACCESSION NO.	3. RECIPIENT'S CATALOG NUMBER
4. TITLE (and Subtitle): OPTIMUM SHAPES OF CENTRAL HOLES IN SQUARE PLATES SUBJECTED TO UNIAXIAL LOAD		5. TYPE OF REPORT & PERIOD COVERED
		6. PERFORMING ORG. REPORT NUMBER
7. AUTHOR(s): A. J. Durelli, M. Erickson and K. Rajaiah		8. CONTRACT OR GRANT NUMBER(s): N00014-81-K-0186
9. PERFORMING ORGANIZATION NAME AND ADDRESS: University of Maryland, College park, Md.		10. PROGRAM ELEMENT, PROJECT, TASK AREA & WORK UNIT NUMBERS
11. CONTROLLING OFFICE NAME AND ADDRESS: Office of Naval Research, Dept. of the Navy, Washington, D.C. 20025		12. REPORT DATE: September 1981
		13. NUMBER OF PAGES: 12
14. MONITORING AGENCY NAME & ADDRESS(if different from Controlling Office)		15. SECURITY CLASS. (of this report)
		15a. DECLASSIFICATION/DOWNGRADING SCHEDULE

16. DISTRIBUTION STATEMENT (of this Report)

Distribution of this report is unlimited

17. DISTRIBUTION STATEMENT (of the abstract entered in Block 20, if different from Report)

18. SUPPLEMENTARY NOTES

19. KEY WORDS (Continue on reverse side if necessary and identify by block number)

Optimization
Holes
Square Plates
Photoelasticity
Stress Concentrations

20. ABSTRACT (Continue on reverse side if necessary and identify by block number)

This paper presents the shapes that will optimize the stress distribution about central holes in square plates subjected to uniform load on two opposite sides of the plate. The study is conducted for a large range of hole to plate widths ratios (D/W). The stress concentration factor for the optimized holes decreased by as much as 21% when compared to the one associated with a circular hole. Simultaneously, the weight of the plate with optimized hole is reduced by as much as 36% as compared to the

DD FORM 1 JAN 73 1473 EDITION OF 1 NOV 65 IS OBSOLETE
S/N 0102-014-6601 |

SECURITY CLASSIFICATION OF THIS PAGE (When Data Entered)

OPTIMIZATION OF HOLE SHAPES IN CIRCULAR CYLINDRICAL SHELLS UNDER AXIAL TENSION

by

K. Rajaiah and A. J. Durelli

Sponsored by

Office of Naval Research
Department of the Navy
Washington, D.C. 20025

on

Contract No. N00014-81-K-0186
U.M. Project No. SF-CARS

Report No. 57

School of Engineering
University of Maryland
College Park, Md. 20742

OPTIMIZATION OF HOLE SHAPES IN CIRCULAR CYLINDRICAL SHELLS UNDER AXIAL TENSION

by

K. Rajaiah and A. J. Durelli

TABLE OF CONTENTS

ABSTRACT . . . . . .

INTRODUCTION . . . . . .

MODEL MAKING . . . . . .

LOADING SYSTEM . . . . . .

TYPE OF POLARISCOPE USED . . . . . .

OPTIMIZATION PROCESS . . . . . .

RESULTS AND DISCUSSION . . . . . .

ACKNOWLEDGMENTS. . . . . .

REFERENCES . . . . . .

Optimization of Hole Shapes in Circular Cylindrical Shells under Axial Tension

Optimization of hole shapes in cylindrical shells under axial tension is obtained using two-dimensional photoelastic and birefringent-coating techniques, resulting in uniform membrane stresses along the tensile and compressive segments of the hole boundary

by K. Rajaiah and A.J. Durelli

ABSTRACT—Hole shapes are optimized in circular cylindrical shells subjected to axial load considering only the predominantly large membrane stresses present around the holes. Two-dimensional photoelastic isochromatics obtained with a special-purpose polariscope are utilized for the optimization process. The process leads to a significant decrease in the membrane stress-concentration factor and a modest decrease in weight, thus yielding a considerable increase in strength-to-weight ratio. This paper presents results for certain typical ratios of hole diameter to shell diameter. Previous theoretical and experimental studies for the circular hole have also been verified.

Introduction

Optimization of hole shapes in engineering structures like plates and shells is important from fatigue and minimum-weight considerations. In a series of papers, Durelli and his associates[1-4] have recently presented a practical way of arriving at optimum hole shapes in uniaxially loaded plates and rings from simple two-dimensional photoelastic experiments by removal of material from low-stress regions around the hole and making an isochromatic fringe coincide separately with the tensile and compressive segments of the boundary. This process leads to a significant reduction in the stress-concentration factor as well. The present paper is an extension of the same concepts to the optimization of hole shapes in circular cylindrical shells under uniaxial tension.

The stress pattern around holes in cylindrical shells is complicated by the fact that both membrane and bending stresses are present. Fortunately, for circular holes in circular cylindrical shells under axial tension, Peterson's[5] handbook shows that membrane stresses (computed by Van Dyke) are predominant on the hole edge while bending stresses are of a much smaller magnitude (Fig. 1). As a percentage of the total stress, the bending stresses constitute less than 16 percent for $t/R > 0.004$ (Fig. 2).

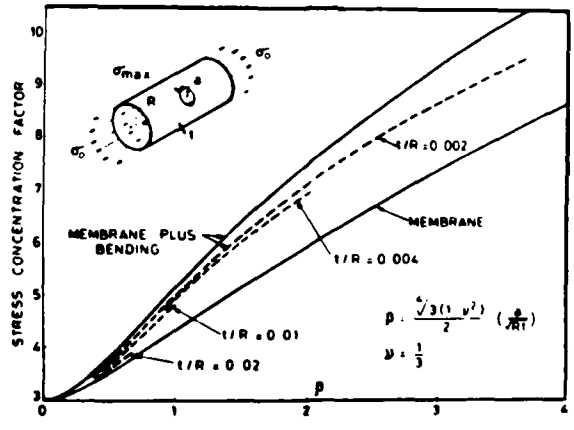

Fig. 1—Membrane and bending stress-concentration factors for circular holes in circular cylindrical shell under axial tension

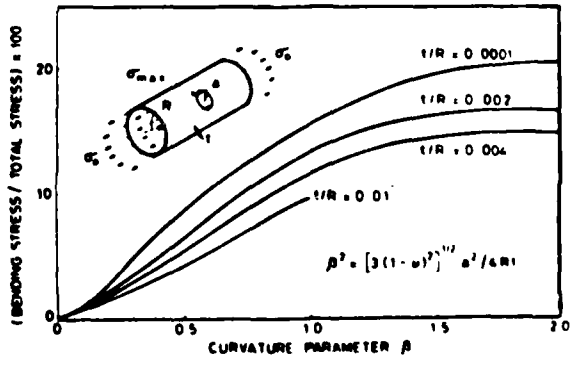

Fig. 2—Percentage of maximum bending stress present around the hole for various curvatures β of the hole

K. Rajaiah (SESA Member) is Professor, Indian Institute of Technology, Powai, Bombay 400 076, India. A.J. Durelli (SESA Honorary Member) is Professor, Department of Mechanical Engineering, University of Maryland, College Park, MD 20742.

Paper was presented at Fourth SESA International Congress on Experimental Mechanics held in Boston, MA on May 25-30.

Original manuscript submitted: August 1, 1980. Authors notified of acceptance: September 19, 1980. Final version received: October 9, 1980.

In an ideal situation, one would attempt to optimize the hole shape considering both the membrane and the bending stresses. Obviously, such an exercise would be quite involved. From a practical-design point of view, it should be enough if the hole shapes are optimized by taking into account only the predominantly large membrane stresses. The method proposed in this paper is based on this idea.

Defining an optimized hole as one in which uniform membrane stresses are present in both the tensile and compressive segments of the hole boundary, it is found that two-dimensional photoelasticity (either by transmission or by reflection) can be used to obtain optimized hole shapes using shell models made of birefringent materials. In the present investigation, this technique is utilized for the optimization of hole shapes in circular cylindrical shells under uniaxial loading. Optimized hole shapes, the corresponding stress-concentration factor and stress distributions around the holes are presented for some typical ratios of hole diameter/shell diameter. The geometric constrain specified for the optimized hole is that the optimized boundary should be in-between the circle of diameter $2a$, and the square of side $2a$.

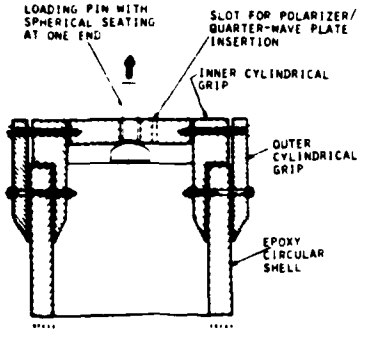

Fig. 3—Loading fixture

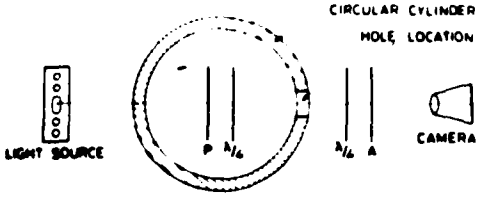

Fig. 4—Transmission-polariscope arrangement

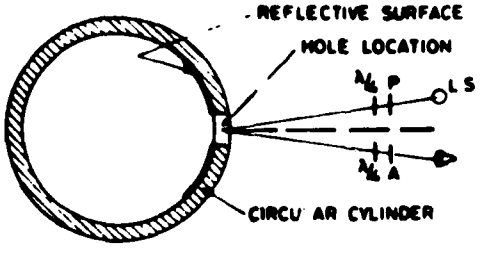

Fig. 5—Reflection-polariscope arrangement

Model Making

Three different types of shells were made. Preliminary experiments used commercially available Perspex tubes of 3-in. (76-mm) nominal diameter with 0.125-in. (3-mm) nominal wall thickness (identified as Type I shell). While the thickness distribution was within 5 percent of the nominal value, the cylinder was not sufficiently straight. Due to this, certain bending effects were observed. The advantage of this material was the negligible time-edge stresses around the hole, but the major problem was the large load required to produce a sufficient number of fringes.

The second set of experiments used shells made of epoxy sheets, 1.3 mm ±0.05 mm thick cast between two substantially thick flat Perspex sheets (identified as Type II shell). Each sheet in a semipolymerized state was cut to size and wrapped around a 50-mm-diam ground-metal cylinder coated with a releasing agent. The edges of the epoxy sheet touching each other were joined together with a 5-mm-wide, very-thin strip providing a bonded butt joint. To provide symmetry to the shell, an identical strip was bonded on the diagonally opposite side. The open ends of the cylindrical shell were reinforced over a distance of 1.0 in. (25 mm) with bonded epoxy strips to provide stiffness near the end fixture. After complete curing, the cylinder was removed and tested. For a no-hole condition, it was verified that there were no residual stresses except very close to the joints, and that the reinforcement affects the stress distribution over the uniform section only to a distance of about twice the shell thickness. Even with the introduction of holes, there were no measurable effects of the reinforcing strips over the hole stress distribution. The advantage of this technique was the fine transmission properties of the shell and absence of machining process.

The last set of experiments were carried out with integrally cast circular cylindrical shells (identified as Type III shell) using a plaster-of-paris mold with a centrally located, slightly tapered metal cylinder coated with a silicone-grease-releasing agent. After complete curing, the inner metal cylinder was first pushed out using a hydraulic press and then the outer plaster-of-paris shell was removed. Both the inner and outer surfaces of the epoxy shell* were turned on a lathe to the required dimensions (50-mm diameter and 0.4 mm thick). The surfaces needed a thin coating of oil to make them transparent. Dimensionally, these cylinders were the best. In the last two experiments, in order to overcome the time-edge effect around the holes, the experiments were carried out immediately after the introduction of the holes. Optimization was also completed on the same day.

The introduction of the circular hole was carried out in different stages starting from a small-diameter hole and progressively increasing it to the required diameter and then finishing with a reamer. The holes were stress free for all practical purposes. The length of all the shells used was sufficient for the ends to have negligible effect on the hole. No creep effects were noticed in any of the shells.

Loading System

Uniform axial loading of both tension and compression types was applied on the models. The compression load

*Material: Dobeckot resin 505C + hardener 758 (10:1) manufactured in India. f = 44.4 lb/in.-fr (7.8 kN/m-fr).

was given through rubber sheet and wooden blocks kept on the model with a 12-mm ball located at the center. The shell could be axially loaded and the uniformity of the stress at some distance away from the load checked.

The tensile load was applied through shear with tightly gripped end rings and a disk with a spherical-ended rod at the center ensuring the alignment of the shell (Fig. 3). In these tests, compression loading was more difficult to control than tensile loading and all the reported results correspond to tensile loading.

Type of Polariscope Used

Conventional transmission polariscopes are clearly unsuitable for the study of the present problem. A polariscope, based on Houghton's experiments,[4] with the polarizer and first quarter-wave plate having their planes parallel to the plane of the hole and located at the center of the shell, was used. A diffused 130-W sodium-vapor lamp was used as light source on one side of the shell while the second quarter-wave plate and the analyzer were located on the other side. The fringes were recorded using a bellows-type camera with a 25-in. (62.5-cm) focal-length lens (Fig. 4).

For the reflection studies, a conventional polariscope of the type shown in Fig. 5 was tried. With this polariscope, the shadow around the hole edge is very pronounced. The results obtained are not very reliable. Due to this difficulty, the reflection method was only used in the present study as an occasional check. A special reflection polariscope of the type used by Slot[5] and, more recently, by Durelli *et al.*[6] would appear to be ideal for this problem. With one polariscope as with the other, only membrane stresses are recorded.

Optimization Process

For optimization, the constraint was stipulated that the boundary of the hole lie between the circle of diameter $2a$ and the square side $2a$. The process followed is very similar to the one mentioned in Refs. 1-4. It starts with the viewing of the isochromatics around the circular hole in the cylinder loaded axially, using the polariscope described above. From a study of the isochromatics, the tensile and compressive segments and the low and high stress regions around the hole boundary are established. The operator starts filing away material from the boundary at the points where the stress is minimum, say, on the tensile segment of the boundary, and with the hole region in view through the analyzer. This operation redistributes the stresses bringing down the maximum stress along that segment. The operation is continued until an isochromatic fringe coincides with the tensile boundary. The same operation is conducted on the other segments.

Results and Discussion

The isochromatic patterns for a typical circular and corresponding optimized holes are shown in Fig. 6. The stress distributions at the boundaries of the holes for three different ratios of hole diameter to shell diameter are presented in Fig. 7. For the sake of comparison, Fig. 7 also includes the distributions corresponding to the circular holes as determined in the present experiments. The empirically developed geometry has been fitted with a combination of circles of different diameters and common tangents at the points of intersections. The geometry of a typical optimized shape is shown in Fig. 8.

Jessop *et al.*[9] have determined the stress-concentration factors in circular tubes with transverse circular holes under tension for some typical values of β and t/R, using the stress-freezing technique. Comparison of their results with the present values, as well as with the analytical results quoted in Ref. 5, shows close agreement. Fig. 9, but are about 5 percent lower.

The condition under which the tests were conducted required that the diameter of the holes used be small. This increased the difficulties of the analysis. It is estimated that the level of precision obtained is 5 percent. The

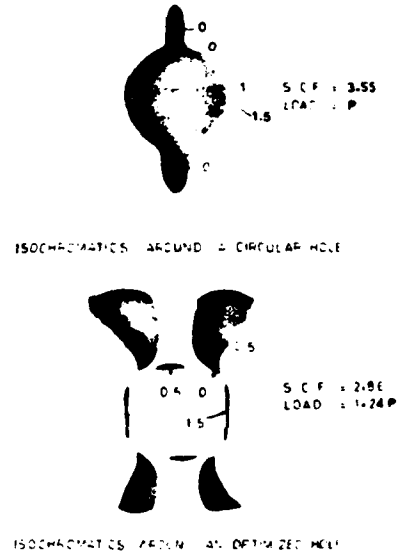

Fig. 6—Isochromatic-fringe patterns around circular and optimized holes in a circular cylindrical shell under axial load (a/R = 0.24; t/R = 0.056)

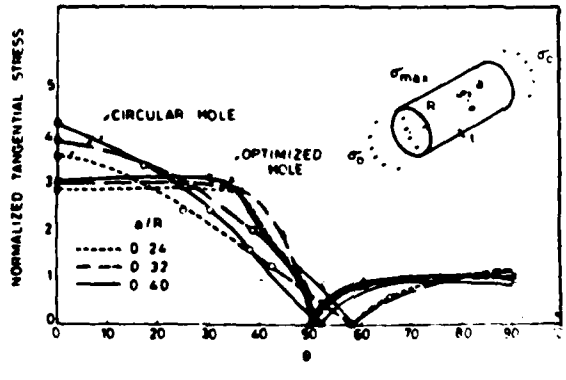

Fig. 7—Stress distribution at the boundary of optimized and circular holes in circular cylindrical shells under axial load (t/R = 0.056)

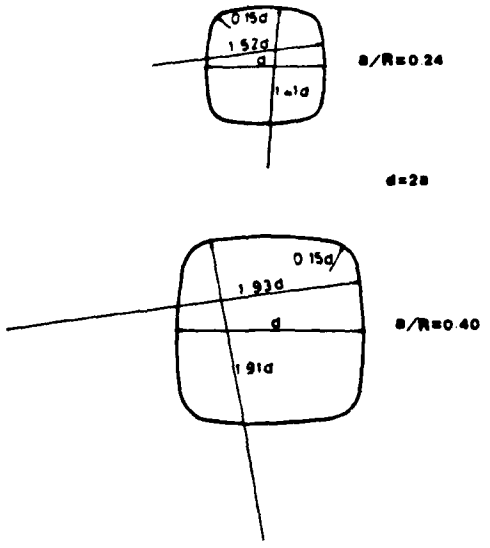

Fig. 8—Optimized geometries of holes for minimum stress-concentration factor in a circular cylindrical shell under axial load

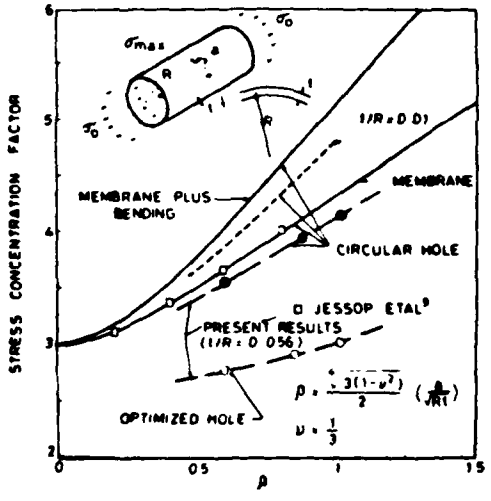

Fig. 9—Stress-concentration factors for a single circular and optimized hole in circular cylindrical shells subjected to axial loading

optimization process is also difficult on small holes.[3] However, the optimized hole shapes and the percentage reduction in stress-concentration factor can be considered to be reliable. For better accuracy, larger hole sizes in large-diameter shells should be used.

In Fig. 9, comparison of the stress-concentration-factor values for circular and optimized holes shows that the optimization process has brought down the stress-concentration factor by as much as 25 percent. The reduction in stress-concentration factor is larger for the large hole sizes. Larger gains can be anticipated for $\beta > 1$. The stress-concentration factor increases with increasing hole diameter for optimized holes also. The optimum hole shapes obtained for the cases investigated are close to a double barrel.

Comparison of the results obtained using shells with (Type II) and without (Type III) reinforcements indicate that, for the range of hole diameters considered, the stress-concentration-factor values in both cases are in close agreement. The optimization process, apart from the reduction in stress-concentration factor has also resulted in a decrease in weight as evidenced by the increase in the hole area in the optimized case. The increase in hole area is found to be of the order of 5 percent to 11 percent. One can conclude that the optimization process has thus led to a significant increase in the strength/weight ratio of the shell.

As mentioned earlier, the hole optimization has been carried out considering only the effect of membrane stresses. Whether this process leads to an increase or decrease of the bending stresses around the hole is not known yet. For a complete understanding of the problem, estimation of the bending stresses for both the circular and optimized shapes would be required, particularly for very thin shells.

As a matter of interest, the shape shown in Fig. 9 for the small hole could be compared to the one developed in Ref. 2, for the case of the large plate under uniaxial loading, and the one developed in Ref. 4 for the case of the large plate subjected to equal biaxial loading of opposite signs. It can be noted that the transverse boundary of the optimized hole in the case of the plate under uniaxial load is flat, rather than curved as in the other two cases. It is possible that further work on the shell case will show that an improvement in optimization can be obtained by using a flatter transverse boundary for the hole.

Acknowledgments

The research program from which this paper was developed was supported, in part, by the Office of Naval Research (Contract No. N00014-76-C-0487). The authors are grateful to N. Perrone and N. Basdekas of ONR for their support. The photoelastic specimens have been prepared by S. Nygren and the manuscript reproduction by P. Baxter.

References

1. Durelli, A.J., Brown, K. and Yee, P., "Optimization of Geometric Discontinuities in Stress Fields," EXPERIMENTAL MECHANICS, **18** (8), 303-308 (Aug. 1978).

2. Durelli, A.J. and Rajaiah, K., "Optimum Hole Shapes in Finite Plates Under Uniaxial Load," J. of Appl. Mech., **46**, 691-695 (Sept. 1979).

3. Durelli, A.J. and Rajaiah, K., "Optimized Inner Boundary Shapes in Circular Rings Under Diametral Compression," Strain, **15**, 127-130 (Oct. 1979).

4. Durelli, A.J. and Rajaiah, K., "Lighter and Stronger," EXPERIMENTAL MECHANICS, **20** (11), 369-380 (Nov. 1980).

5. Peterson, R.E., "Stress Concentration Factors," Wiley Interscience (1974).

6. Houghton, D.S., "Stress Concentration Around Cut-outs in a Cylinder," J. of the Royal Aeron. Soc., **65**, 201-204 (1961).

7. Slot, T., "Reflection Polariscope for Photography of Photoelastic Coatings," EXPERIMENTAL MECHANICS, **2** (2), 41-47 (1962).

8. Durelli, A.J. and Rajaiah, K., "Determination of Strains in Photoelastic Coatings," EXPERIMENTAL MECHANICS, **20** (2), 57-64 (1980).

9. Jessop, H.T., Snell, C. and Allison, J.M., "The Stress Concentration Factors in Circular Tubes with Transverse Circular Holes," Aeronautical Quarterly, **10**, 326-341 (1959).

SECURITY CLASSIFICATION OF THIS PAGE (When Data Entered)

REPORT DOCUMENTATION PAGE		READ INSTRUCTIONS BEFORE COMPLETING FORM
1. REPORT NUMBER 57	2. GOVT ACCESSION NO.	3. RECIPIENT'S CATALOG NUMBER
4. TITLE (and Subtitle) OPTIMIZATION OF HOLE SHAPES IN CIRCULAR CYLINDRICAL SHELLS UNDER AXIAL TENSION		5. TYPE OF REPORT & PERIOD COVERED 6. PERFORMING ORG. REPORT NUMBER
7. AUTHOR(s) K. Rajaiah and A. J. Durelli		8. CONTRACT OR GRANT NUMBER(s) N00014-81-K-0186
9. PERFORMING ORGANIZATION NAME AND ADDRESS University of Maryland College Park, Md.		10. PROGRAM ELEMENT, PROJECT, TASK AREA & WORK UNIT NUMBERS
11. CONTROLLING OFFICE NAME AND ADDRESS Office of Naval Research Dept. of the Navy, Washington D.C. 20025		12. REPORT DATE September 1981 13. NUMBER OF PAGES 12
14. MONITORING AGENCY NAME & ADDRESS(if different from Controlling Office)		15. SECURITY CLASS. (of this report) 15a. DECLASSIFICATION/DOWNGRADING SCHEDULE

16. DISTRIBUTION STATEMENT (of this Report)

Distribution of this report is unlimited

17. DISTRIBUTION STATEMENT (of the abstract entered in Block 20, if different from Report)

18. SUPPLEMENTARY NOTES

19. KEY WORDS (Continue on reverse side if necessary and identify by block number)

Optimization
Shells
Holes
Stress Concentration
Photoelasticity

20. ABSTRACT (Continue on reverse side if necessary and identify by block number)

Hole shapes are optimized in circular cylindrical shells subjected to axial load considering only the predominantly large membrane stresses present around the holes. Two dimensional photoelastic isochromatics obtained with a special purpose polariscope are utilized for the optimization process. The process leads to a significant decrease in the membrane s.c.f. and a modest decrease in weight, thus yielding a considerable increase in strength to weight ratio. This paper presents results for certain typical ratios of hole diameter to

DD FORM 1 JAN 73 1473 EDITION OF 1 NOV 65 IS OBSOLETE
S/N 0102-014-6601 |

SECURITY CLASSIFICATION OF THIS PAGE (When Data Entered)

circular hole. Coefficient of efficiency of around 0.92 is achieved for all D/W ratios. The geometry of the optimized holes are presented in a form suitable for use by designers.

Part 1 - Government
Administrative and Liaison Activities

Office of Naval Research
Department of the Navy
Arlington, Virginia 22217
Attn: Code 474 (2)
Code 471
Code 200

Director
Office of Naval Research
Branch Office
666 Summer Street
Boston, Massachusetts 02210

Director
Office of Naval Research
Branch Office
536 South Clark Street
Chicago, Illinois 60605

Director
Office of Naval Research
New York Area Office
715 Broadway - 5th Floor
New York, New York 10003

Director
Office of Naval Research
Branch Office
1030 East Green Street
Pasadena, California 91106

Naval Research Laboratory (6)
Code 2627
Washington, D.C. 20375

Defense Documentation Center (12)
Cameron Station
Alexandria, Virginia 22314

Navy

Undersea Explosion Research Division
Naval Ship Research and Development
Center
Norfolk Naval Shipyard
Portsmouth, Virginia 23709
Attn: Dr. E. Palmer, Code 177

Naval Research Laboratory
Washington, D.C. 20375
Attn: Code 8400
8410
8430
8440
6300
6390
6380

David W. Taylor Naval Ship Research
and Development Center
Annapolis, Maryland 21402
Attn: Code 2740
28
281

Naval Weapons Center
China Lake, California 93555
Attn: Code 4062
4520

Commanding Officer
Naval Civil Engineering Laboratory
Code L31
Port Hueneme, California 93041

Naval Surface Weapons Center
White Oak
Silver Spring, Maryland 20910
Attn: Code R-10
G-402
K-82

Technical Director
Naval Ocean Systems Center
San Diego, California 92152

Navy (Con't.)

Supervisor of Shipbuilding
U.S. Navy
Newport News, Virginia 23607

Navy Underwater Sound
Reference Division
Naval Research Laboratory
P.O. Box 8337
Orlando, Florida 32806

Chief of Naval Operations
Department of the Navy
Washington, D.C. 20350
Attn: Code OP-098

Strategic Systems Project Office
Department of the Navy
Washington, D.C. 20376
Attn: NSP-200

Naval Air Systems Command
Department of the Navy
Washington, D.C. 20361
Attn: Code 5302 (Aerospace and Structures)
604 (Technical Library)
320B (Structures)

Naval Air Development Center
Warminster, Pennsylvania 18974
Attn: Aerospace Mechanics
Code 606

U.S. Naval Academy
Engineering Department
Annapolis, Maryland 21402

Naval Facilities Engineering Command
200 Stovall Street
Alexandria, Virginia 22332
Attn: Code 03 (Research and Development)
04B
045
14114 (Technical Library)

Naval Sea Systems Command
Department of the Navy
Washington, D.C. 20362
Attn: Code 05H
312
322
323
05R
32R

Commander and Director
David W. Taylor Naval Ship
Research and Development Center
Bethesda, Maryland 20084
Attn: Code 042
17
172
173
174
1800
1844
012.2
1900
1901
1945
1960
1962

Naval Underwater Systems Center
Newport, Rhode Island 02840
Attn: Dr. R. Trainor

Naval Surface Weapons Center
Dahlgren Laboratory
Dahlgren, Virginia 22448
Attn: Code G04
G20

Technical Director
Mare Island Naval Shipyard
Vallejo, California 94592

Navy (Con't.)

U.S. Naval Postgraduate School
Library
Code 0384
Monterey, California 93940

Webb Institute of Naval Architecture
Attn: Librarian
Crescent Beach Road, Glen Cove
Long Island, New York 11542

Army

Commanding Officer (2)
U.S. Army Research Office
P.O. Box 12211
Research Triangle Park, NC 27709
Attn: Mr. J. J. Murray, CRD-AA-IP

Watervliet Arsenal
MAGGS Research Center
Watervliet, New York 12189
Attn: Director of Research

U.S. Army Materials and Mechanics
Research Center
Watertown, Massachusetts 02172
Attn: Dr. R. Shea, DRXMR-T

U.S. Army Missile Research and
Development Center
Redstone Scientific Information
Center
Chief, Document Section
Redstone Arsenal, Alabama 35809

Army Research and Development
Center
Fort Belvoir, Virginia 22060

NASA

National Aeronautics and Space
Administration
Structures Research Division
Langley Research Center
Langley Station
Hampton, Virginia 23365

National Aeronautics and Space
Administration
Associate Administrator for Advanced
Research and Technology
Washington, D.C. 20546

Air Force

Wright-Patterson Air Force Base
Dayton, Ohio 45433
Attn: AFFDL (FB)
(FBR)
(FBE)
(FBS)
AFML (MBM)

Chief Applied Mechanics Group
U.S. Air Force Institute of Technology
Wright-Patterson Air Force Base
Dayton, Ohio 45433

Chief, Civil Engineering Branch
WLRC, Research Division
Air Force Weapons Laboratory
Kirtland Air Force Base
Albuquerque, New Mexico 87117

Air Force Office of Scientific Research
Bolling Air Force Base
Washington, D.C. 20332
Attn: Mechanics Division

Department of the Air Force
Air University Library
Maxwell Air Force Base
Montgomery, Alabama 36112

Other Government Activities

Commandant
Chief, Testing and Development Division
U.S. Coast Guard
1300 E Street, NW.
Washington, D.C. 20226

Technical Director
Marine Corps Development
and Education Command
Quantico, Virginia 22134

Director Defense Research
and Engineering
Technical Library
Room 3C128
The Pentagon
Washington, D.C. 20301

Dr. M. Gaus
National Science Foundation
Environmental Research Division
Washington, D.C. 20550

Library of Congress
Science and Technology Division
Washington, D.C. 20540

Director
Defense Nuclear Agency
Washington, D.C. 20305
Attn: SPSS

Mr. Jerome Persh
Staff Specialist for Materials
and Structures
OUSDR&E, The Pentagon
Room 3D1089
Washington, D.C. 20301

Chief, Airframe and Equipment Branch
FS-120
Office of Flight Standards
Federal Aviation Agency
Washington, D.C. 20553

National Academy of Sciences
National Research Council
Ship Hull Research Committee
2101 Constitution Avenue
Washington, D.C. 20418
Attn: Mr. A. R. Lytle

National Science Foundation
Engineering Mechanics Section
Division of Engineering
Washington, D.C. 20550

Picatinny Arsenal
Plastics Technical Evaluation Center
Attn: Technical Information Section
Dover, New Jersey 07801

Maritime Administration
Office of Maritime Technology
14th and Constitution Avenue, NW.
Washington, D.C. 20230

Universities

Dr. J. Tinsley Oden
University of Texas at Austin
345 Engineering Science Building
Austin, Texas 78712

Professor Julius Miklowitz
California Institute of Technology
Division of Engineering
and Applied Sciences
Pasadena, California 91109

Dr. Harold Liebowitz, Dean
School of Engineering and
Applied Science
George Washington University
Washington, D.C. 20052

Professor Eli Sternberg
California Institute of Technology
Division of Engineering and
Applied Sciences
Pasadena, California 91109

Professor Paul M. Naghdi
University of California
Department of Mechanical Engineering
Berkeley, California 94720

Professor A. J. Durelli
Oakland University
School of Engineering
Rochester, Missouri 48063

Professor F. L. DiMaggio
Columbia University
Department of Civil Engineering
New York, New York 10027

Professor Norman Jones
The University of Liverpool
Department of Mechanical Engineering
P. O. Box 147
Brownlow Hill
Liverpool L69 3BX
England

Professor E. J. Skudrzyk
Pennsylvania State University
Applied Research Laboratory
Department of Physics
State College, Pennsylvania 16801

Professor J. Klosner
Polytechnic Institute of New York
Department of Mechanical and
Aerospace Engineering
333 Jay Street
Brooklyn, New York 11201

Professor R. A. Schapery
Texas A&M University
Department of Civil Engineering
College Station, Texas 77843

Professor Walter D. Pilkey
University of Virginia
Research Laboratories for the
Engineering Sciences and
Applied Sciences
Charlottesville, Virginia 22901

Professor K. D. Willmert
Clarkson College of Technology
Department of Mechanical Engineering
Potsdam, New York 13676

Professor R. S. Rivlin
Lehigh University
Center for the Application
of Mathematics
Bethlehem, Pennsylvania 18015

Universities (Con't

Dr. Walter E. Haisler
Texas A&M University
Aerospace Engineering Department
College Station, Texas 77843

Dr. Hussein A. Kamel
University of Arizona
Department of Aerospace and
Mechanical Engineering
Tucson, Arizona 85721

Dr. S. J. Fenves
Carnegie-Mellon University
Department of Civil Engineering
Schenley Park
Pittsburgh, Pennsylvania 15213

Dr. Ronald L. Huston
Department of Engineering Analysis
University of Cincinnati
Cincinnati, Ohio 45221

Professor G. C. M. Sih
Lehigh University
Institute of Fracture and
Solid Mechanics
Bethlehem, Pennsylvania 18015

Professor Albert S. Kobayashi
University of Washington
Department of Mechanical Engineering
Seattle, Washington 98105

Professor Daniel Frederick
Virginia Polytechnic Institute and
State University
Department of Engineering Mechanics
Blacksburg, Virginia 24061

Professor A. C. Eringen
Princeton University
Department of Aerospace and
Mechanical Sciences
Princeton, New Jersey 08540

Professor E. H. Lee
Stanford University
Division of Engineering Mechanics
Stanford, California 94305

Professor Albert I. King
Wayne State University
Biomechanics Research Center
Detroit, Michigan 48202

Dr. V. R. Hodgson
Wayne State University
School of Medicine
Detroit, Michigan 48202

Dean B. A. Boley
Northwestern University
Department of Civil Engineering
Evanston, Illinois 60201

Professor H. W. Liu
Syracuse University
Department of Chemical Engineering
and Metallurgy
Syracuse, New York 13210

Professor S. Bodner
Technion R&D Foundation
Haifa, Israel

Professor Werner Goldsmith
University of California
Department of Mechanical Engineering
Berkeley, California 94720

Universities (Con't)

Professor P. G. Hodge, Jr.
University of Minnesota
Department of Aerospace Engineering
and Mechanics
Minneapolis, Minnesota 55455

Dr. D. C. Drucker
University of Illinois
Dean of Engineering
Urbana, Illinois 61801

Professor N. M. Newmark
University of Illinois
Department of Civil Engineering
Urbana, Illinois 61803

Professor E. Reissner
University of California, San Diego
Department of Applied Mechanics
La Jolla, California 92037

Professor William A. Nash
University of Massachusetts
Department of Mechanics and
Aerospace Engineering
Amherst, Massachusetts 01002

Professor G. Herrmann
Stanford University
Department of Applied Mechanics
Stanford, California 94305

Professor J. D. Achenbach
Northwest University
Department of Civil Engineering
Evanston, Illinois 60201

Professor S. B. Dong
University of California
Department of Mechanics
Los Angeles, California 90024

Professor Burt Paul
University of Pennsylvania
Towne School of Civil and
Mechanical Engineering
Philadelphia, Pennsylvania 19104

Professor F. A. Cozzarelli
State University of New York at
Buffalo
Division of Interdisciplinary Studies
Karr Parker Engineering Building
Chemistry Road
Buffalo, New York 14214

Professor Joseph L. Rose
Drexel University
Department of Mechanical Engineering
and Mechanics
Philadelphia, Pennsylvania 19104

Professor B. K. Donaldson
University of Maryland
Aerospace Engineering Department
College Park, Maryland 20742

Professor Joseph A. Clark
Catholic University of America
Department of Mechanical Engineering
Washington, D.C. 20064

Dr. Samuel B. Batdorf
University of California
School of Engineering
and Applied Science
Los Angeles, California 90024

Professor Isaac Fried
Boston University
Department of Mathematics
Boston, Massachusetts 02215

Universities (Con't)

Professor E. Krempl
Rensselaer Polytechnic Institute
Division of Engineering
Engineering Mechanics
Troy, New York 12181

Dr. Jack R. Vinson
University of Delaware
Department of Mechanical and Aerospace
Engineering and the Center for
Composite Materials
Newark, Delaware 19711

Dr. J. Duffy
Brown University
Division of Engineering
Providence, Rhode Island 02912

Dr. J. L. Swedlow
Carnegie-Mellon University
Department of Mechanical Engineering
Pittsburgh, Pennsylvania 15213

Dr. V. K. Varadan
Ohio State University Research Foundation
Department of Engineering Mechanics
Columbus, Ohio 43210

Dr. Z. Hashin
University of Pennsylvania
Department of Metallurgy and
Materials Science
College of Engineering and
Applied Science
Philadelphia, Pennsylvania 19104

Dr. Jackson C. S. Yang
University of Maryland
Department of Mechanical Engineering
College Park, Maryland 20742

Professor T. Y. Chang
University of Akron
Department of Civil Engineering
Akron, Ohio 44325

Professor Charles W. Bert
University of Oklahoma
School of Aerospace, Mechanical,
and Nuclear Engineering
Norman, Oklahoma 73019

Professor Satya N. Atluri
Georgia Institute of Technology
School of Engineering and
Mechanics
Atlanta, Georgia 30332

Professor Graham F. Carey
University of Texas at Austin
Department of Aerospace Engineering
and Engineering Mechanics
Austin, Texas 78712

Dr. S. S. Wang
University of Illinois
Department of Theoretical and
Applied Mechanics
Urbana, Illinois 61801

Industry and Research Institutes

Dr. Norman Hobbs
Kaman AviDyne
Division of Kaman
Sciences Corporation
Burlington, Massachusetts 01803

Argonne National Laboratory
Library Services Department
9700 South Cass Avenue
Argonne, Illinois 60440

Industry and Research Institutes (Con't)

Dr. M. C. Junger
Cambridge Acoustical Associates
54 Rindge Avenue Extension
Cambridge, Massachusetts 02140

Dr. V. Godino
General Dynamics Corporation
Electric Boat Division
Groton, Connecticut 06340

Dr. J. E. Greenspon
J. G. Engineering Research Associates
3831 Menlo Drive
Baltimore, Maryland 21215

Newport News Shipbuilding and
Dry Dock Company
Library
Newport News, Virginia 23607

Dr. W. F. Bozich
McDonnell Douglas Corporation
5301 Bolsa Avenue
Huntington Beach, California 92647

Dr. H. N. Abramson
Southwest Research Institute
8500 Culebra Road
San Antonio, Texas 78284

Dr. R. C. DeHart
Southwest Research Institute
8500 Culebra Road
San Antonio, Texas 78284

Dr. M. L. Baron
Weidlinger Associates
110 East 59th Street
New York, New York 10022

Dr. T. L. Geers
Lockheed Missiles and Space Company
3251 Hanover Street
Palo Alto, California 94304

Mr. William Caywood
Applied Physics Laboratory
Johns Hopkins Road
Laurel, Maryland 20810

Dr. Robert E. Duncan
Pacifica Technology
P.O. Box 148
Del Mar, California 92014

Dr. M. F. Kanninen
Battelle Columbus Laboratories
505 King Avenue
Columbus, Ohio 43201

Dr. A. A. Hoenraim
Daedalean Associates, Inc.
Springlake Research Road
15110 Frederick Road
Woodbine, Maryland 21797

Dr. James W. Jones
Swanson Service Corporation
P.O. Box 5418
Huntington Beach, California 92646

Dr. Robert E. Nickell
Applied Science and Technology
3344 North Torrey Pines Court
Suite 220
La Jolla, California 92037

Dr. Kevin Thomas
Westinghouse Electric Corp.
Advanced Reactors Division
P. O. Box 158
Madison, Pennsylvania 15663


ATE
LME